Enhanced Resilient Fuzzy Stabilization of Discrete-Time Takagi–Sugeno Systems Based on Augmented Time-Variant Matrix Approach

Xiangpeng Xie, *Member, IEEE*, Lei Wan, Zhou Gu, *Member, IEEE*, Dong Yue, *Fellow, IEEE*, and Jiayue Sun, *Associate Member, IEEE*

***Abstract*—In this technical correspondence, the resilient fuzzy stabilization is enhanced in the direction of elevating the feasible stabilization region as large as possible while the same alert threshold is chosen as the recent one. To do this, the switching-type fuzzy state-feedback controller is designed with a set of switch modes so that more groups of gain matrices can be introduced to enhance the degree of freedom. What is far more important is that a novel augmented time-variant matrix approach is proposed in order to collect the proprietary features of normalized fuzzy weighting functions with regard to each switch mode. Then, all the obtained augmented time-variant matrices are split into a set of positive/negative matrices, which can be elaborately assigned into different monomials of our designing conditions under the framework of homogeneous polynomials. Therefore, less conservative results of resilient fuzzy stabilization are obtained even if some higher alert thresholds are chosen for probably ensuring the establishment of the involved precondition. Finally, the superiority of our approach is validated by giving some detailed comparisons on the benchmark example.**

***Index Terms*—Alert threshold, fuzzy systems, nonlinear systems, resilient control.**

I. Introduction

Nonlinear dynamics are often difficult to be addressed and thus, considerable intelligent control methods have been proposed for the sake of providing satisfactory solutions, for example, [1]–[6]. Recently, Takagi–Sugeno (T–S) fuzzy models [7] have attracted special research attention due to their excellent nonlinear modeling characteristics [8]. Based on the T–S fuzzy models, several issues of nonlinear control have been well investigated by using the Lyapunov direct methods [9]–[11]. The first thing of T–S fuzzy control is the issue of fuzzy stabilization [12]. Nevertheless, it has been announced in [13] that two important aspects about fuzzy stabilization are not well solved until now, that is: 1) how to achieve feasible designing conditions with less conservativeness as possible? and 2) how to give a real-time controller by spending smaller implementation cost as possible?

At the beginning of related studies, the issue of fuzzy stabilization was tackled by using an intuitive strategy of parallel distributed compensation (PDC), which turned out to be too conservative in most cases. Despite that early results have been relaxed by using various methods, for example, method of set theory [14], methods of local stabilization [15], [16], method of tensor product transformation [17], and methods of piecewise Lyapunov functions [18], [19], those PDC-based designing conditions are still very conservative. As a key progress, the non-PDC control strategy was given in [20] and its extended results [21], [22] showed a great ability in reducing conservativeness via choosing a higher order of gain matrices. In recent years, the method of homogeneous polynomials developed in [23] has been exploited ceaselessly in the direction of deriving feasible designing conditions with less and less conservativeness [24]–[28]. However, for those conventional fuzzy stabilizations, the conservativeness is reduced at the expense of too expensive implementation cost [29]. Despite all this, for conventional fuzzy stabilizations of the well-known benchmark example in this field (example in Section IV), the obtained enhanced quality of reducing conservativeness seems not obvious. That is to say, two important aspects discussed in [13] cannot be solved simultaneously by means of those existing methods of conventional fuzzy stabilization. More recently, a kind of resilient fuzzy stabilization has been proposed in [30] in which an ideal solution to the above challenge is developed preliminarily. In [30], the variation boundary of adjacent-time normalized fuzzy weighting functions (NFWFs) is detected and compared with an alert threshold in real time. But, if a very higher alert threshold is chosen for increasing the establishment possibility of precondition of resilient fuzzy stabilization, then the result of [30] may even become much more conservative than those conventional fuzzy stabilizations [27]–[29]. Therefore, it is meaningful for enlarging the feasible stabilization region as large as possible (i.e., reducing conservativeness) while the same alert threshold is chosen as before.

In this study, the resilient fuzzy stabilization will be enhanced in the direction of enlarging the feasible stabilization region as large as possible while the same alert threshold is chosen as the recent one of [30]. The main contributions of this technical correspondence are listed as follows.

1) Compared to the recent method given in [30], a switching-type fuzzy state-feedback controller is proposed with $2r$ switch modes (r is the number of fuzzy rules), which is much more flexible for enlarging the feasible stabilization region by considering the proprietary features of NFWFs with regard to each switch mode, respectively.
2) For each switch mode, a group ofaugmented time-variant matrices is built for integrating its proprietary features into stability analysis of the closed-loop system. Thus, the obtained augmented time-variant matrices are split into several positive/negative matrices, which can be elaborately assigned into different monomials of our designing conditions under the framework of homogeneous polynomials. Therefore, all the proprietary features can be employed to full advantage in this study.

Benefit from the above measures, the feasible stabilization the region can be evidently enlarged without sacrificing the possibility of

Manuscript received 30 March 2022; accepted 26 May 2022. Date of publication 20 June 2022; date of current version 17 January 2024. This work was supported in part by the National Natural Science Foundation of China under Grant 62022044 and Grant 61773221, and in part by the Jiangsu Natural Science Foundation for Distinguished Young Scholars under Grant BK20190039. This article was recommended by Associate Editor C.-F. Juang. *(Corresponding author: Xiangpeng Xie.)*

Xiangpeng Xie, Lei Wan, and Dong Yue are with the Institute of Advanced Technology, Nanjing University of Posts and Telecommunications, Nanjing 210023, China (e-mail: xiexiangpeng1953@163.com; medongy@vip.163.com).

Zhou Gu is with the College of Mechanical and Electronic Engineering, Nanjing Forestry University, Nanjing 210037, China (e-mail: gzh1808@163.com).

Jiayue Sun is with the School of Information Science and Engineering, Northeastern University, Shenyang 110004, China.

Color versions of one or more figures in this article are available at https://doi.org/10.1109/TCYB.2022.3179048.

Digital Object Identifier 10.1109/TCYB.2022.3179048

the establishment of the precondition for resilient fuzzy stabilization (i.e., the same or even a higher alert threshold is chosen as/than the one applied in [30]).

Notations: Throughout this article, all used notations will be the same as our cited literature. For example, $n!$ is the factorial of the given natural number n. $\mathrm{He}(W) = W + W^T$.

II. Problem Description

A. Discrete-Time T–S Fuzzy Systems

Consider the discrete-time T–S fuzzy systems, which is composed of a batch of If-Then rules [7].

If-Then Rule Indexed by j: If $\varpi_1(t) = \mathcal{M}_1^j, \ldots, \varpi_{n_\varpi}(t) = \mathcal{M}_{n_\varpi}^j$, Then

$$x(t+1) = A_j x(t) + B_j u(t), \qquad 1 \le j \le r$$

where $x(t) \in \mathbb{R}^{n_x}$ is the state vector, $u(t) \in \mathbb{R}^{n_u}$ is the input vector, $\varpi(t) = (\varpi_1(t), \ldots, \varpi_{n_\varpi}(t))^T$ is the involved fuzzy premise vector, and $n_x, n_u, n_\varpi \in \mathbb{Z}_+$.

By means of the sector nonlinearity approach of [7], the overall discrete-time T–S fuzzy system can be written as

$$\begin{aligned} x(t+1) &= \sum_{1\le j\le r} h_j(\varpi(t))(A_j + B_j u(t)) \\ &= A_{\varpi(t)} x(t) + B_{\varpi(t)} u(t) \end{aligned} \tag{1}$$

where $h_j(\varpi(t))$ is the jth NFWF at the current sampling point and one obtains: $h_j(\varpi(t)) \ge 0$, $\sum_{1\le j\le r} h_j(\varpi(t)) = 1$. Moreover, $A_{\varpi(t)} = \sum_{1\le j\le r} h_j(\varpi(t)) A_j$, $B_{\varpi(t)} = \sum_{1\le j\le r} h_j(\varpi(t)) B_j$.

Lemma 1 [31]: Considering $\xi \in \mathbb{R}^{n_a}$, $\Xi \in \mathbb{R}^{n_a \times n_a}$, $E \in \mathbb{R}^{n_b \times n_a}$, $\mathrm{rank}(E) < n_a$, one obtains $\xi^T \Upsilon \xi < 0$ $\forall \xi \ne 0$, with $E\xi = 0$. If and only if $\exists \Phi \in \mathbb{R}^{n_a \times n_b}$ such that $\Xi + \mathrm{He}(\Phi E) < 0$.

B. Preliminaries

A batch of notations for homogeneous polynomials is provided as previous ones in [30] and the references therein.

Given $k_i \in \mathbb{N}$ with $i \in \{1, \ldots, r\}$, $k = k_1 \cdots k_r$ stands for a r-tuple, and $\mathcal{K}(n)$ means the set of r-tuples composed of all k with $\sum_{i=1}^r k_i = n$, $n \in \mathbb{Z}_+$ and the number of elements for $\mathcal{K}(n)$ is $J(n) = [(r+n-1)!/n!(r-1)!]$. $h(\varpi(t))^k = \prod_{i=1}^r h_i(\varpi(t))^{k_i}$ is the monomial while the matrix M_k is a matrix-valued coefficient. For $p \in \mathcal{K}(n)$, one has $\pi(p) = \prod_{i=1}^r (p_i!)$ and $\chi_l = 0 \cdots \underbrace{1}_{l\text{-th}} \cdots 0$. If p and q are two r-tuples, one defines $p - q \ge 0$ if $p_i - q_i \ge 0$ is satisfied for all $i \in \{1, \ldots, r\}$. Two operations of summation $(p+q)$ and subtraction $(p-q)$ should be operated componentwise. Moreover, several simplifications will be employed as follows:

$$\begin{cases} h_j(t) = h_j(\varpi(t)), \ h(t) = (h_1(\varpi(t)), \ldots, h_r(\varpi(t)))^T \\ h(t)^{p\pm q} = \prod_{j=1}^r \left(h_j(\varpi(t))^{p_j \pm q_j}\right), \ h(t-1) = h(\varpi(t-1)). \end{cases} \tag{2}$$

To facilitate understanding, several illustrative examples are shown here. If $r = 4$, $p = p_1p_2p_3p_4 = 2021 \in \mathcal{K}(5)$, $q = q_1q_2q_3q_4 = 1001 \in \mathcal{K}(2)$, $h_1(t) = 0.4, h_2(t) = 0.4, h_3(t) = 0.1, h_4(t) = 0.1$, then one obtains $h(t)^q = 0.4^1 \times 0.4^0 \times 0.1^0 \times 0.1^1 = 0.04$, $p+q = 2021 + 1001 = 3022$, and $p - q = 2021 - 1001 = 1020$.

Furthermore, all the elements of $p \in \mathcal{K}(s)$ can be reordered as $p^1, p^2, \ldots, p^{J(s)}$ in descending order of their corresponding decimal numbers. Such as, for $p \in \mathcal{K}(2)$, $r = 3$, one obtains $p^1 = 200, p^2 = 110, p^3 = 101, p^4 = 020, p^5 = 011$, and $p^6 = 002$. Thus, the augmented matrix composed of all R_{pq} with $p, q \in \mathcal{K}(s)$ is displayed as follows:

$$[W_{pq}]_{J(s)\times J(s)} = \begin{bmatrix} W_{p^1q^1} & \cdots & W_{p^1q^{J(s)}} \\ \vdots & \ddots & \vdots \\ W_{p^{J(s)}q^1} & \cdots & W_{p^{J(s)}q^{J(s)}} \end{bmatrix}.$$

Such as, for $p, q \in \mathcal{K}(2)$, $r = 2$, one obtains

$$[W_{pq}]_{J(2)\times J(2)} = \begin{bmatrix} W_{2020} & W_{2011} & W_{2002} \\ W_{1120} & W_{1111} & W_{1102} \\ W_{0220} & W_{0211} & W_{0202} \end{bmatrix}.$$

Property 1: Consider $\hat{n}, s \in \mathbb{Z}_+$ and $\hat{n} \ge 2s+1$, a scalar μ, matrices U_{pq}^m and Z_{pq}^{mi} for $p, q \in \mathcal{K}(s)$, $m, i \in \{1, \ldots, r\}$ and $i \ne m$, one can obtain two equalities

$$\begin{aligned} &\left(h_m(t) - \mu \sum_{\binom{i\in\{1,\ldots,r\}}{i\ne m}} h_i(t)\right)\left(\sum_{p,q\in\mathcal{K}(s)} h(t)^{p+q} U_{pq}^m\right) \\ &= \sum_{k'\in\mathcal{K}(\hat{n})} \left\{ h(t)^{k'} \left(\sum_{\binom{j\in\{1,\ldots,r\},p,q\in\mathcal{K}(s)}{k''\ge p-q-\chi_j}} \tilde{\Lambda}_{k'pq}^{mj} \right) \right\} \\ &\sum_{\binom{i\in\{1,\ldots,r\}}{i\ne m}} \left\{ (h_m(t) - h_i(t)) \left(\sum_{p,q\in\mathcal{K}(s)} h(t)^{p+q} Z_{pq}^{mi} \right) \right\} \end{aligned} \tag{3}$$

$$= \sum_{k'\in\mathcal{K}(\hat{n})} \left\{ h(t)^{k'} \left(\sum_{\binom{j\in\{1,\ldots,r\},p,q\in\mathcal{K}(s)}{k'-p-q-\chi_j\ge 0}} \bar{\Lambda}_{k'pq}^{mj} \right) \right\} \tag{4}$$

$$\text{where } \tilde{\Lambda}_{k'pq}^{mj} = \begin{cases} \frac{(\hat{n}-2s-1)!}{\pi(k'-p-q-\chi_j)} U_{pq}^m, & \text{for } j = m \\ -\mu \frac{(\hat{n}-2s-1)!}{\pi(k'-p-q-\chi_j)} U_{pq}^m, & \text{for } j \ne m \end{cases}$$

$$\bar{\Lambda}_{k'pq}^{mj} = \begin{cases} \frac{(\hat{n}-2s-1)!}{\pi(k''-p-q-\chi_j)} \sum_{i\in\{1,\ldots,r\}, i\ne m} Z_{pq}^{mi}, & \text{for } j = m \\ -\frac{(\hat{n}-2s-1)!}{\pi(k''-p-q-\chi_j)} Z_{pq}^{mj}, & \text{for } j \ne m. \end{cases}$$

C. Precondition of Resilient Fuzzy Stabilization

Similar to [30], the variation boundary between $h(t-1)$ and $h(t)$ can be expressed as the alert threshold γ in terms of the following assumption.

Assumption 1: Consider the system (1), there does exist an alert threshold $\gamma > 0$, such that the precondition of resilient fuzzy stabilization is ensured for each sampling instant t

$$\gamma(t) = \frac{x^T(t)(P_n(t))^{-1}x(t)}{x^T(t)(P_n(t-1))^{-1}x(t)} \le \gamma. \tag{5}$$

In (5), we define $P_n(t-1) = \sum_{k\in\mathcal{K}(n)} \left\{ h(t-1)^k P_k \right\}$ and $P_n(t) = \sum_{k\in\mathcal{K}(n)} \left\{ h(t)^k P_k \right\}$, respectively, and one has $P_k \in \mathbb{R}^{n_x \times n_x}$, $n \in \mathbb{Z}_+$.

Remark 1: The establishment of the given precondition (5) can be easily checked since all the elements in $\gamma(t)$ are available at each sampling instant. Indeed, Assumption 1 will play an important role in the following proof of Theorem 1, where the resilient fuzzy stabilization can be enhanced in the direction of elevating the feasible stabilization region as large as possible while the same alert threshold of γ is chosen as the recent one of [30].

III. Main Results

Different from [30], the switching-type fuzzy state-feedback controller is designed with $2r$ switch modes (recorded as $m\pm$ for $m \in \{1, \ldots, r\}$) so that more groups of gain matrices can be introduced to enhance the degree of freedom:

$$u(t) = Q_n^{m\pm}(t)\left(S_n^{m\pm}(t)\right)^{-1} x(t) \tag{6}$$

where one has $Q_n^{m\pm}(t) = \sum_{k\in\mathcal{K}(n)} \{h(t)^k Q_k^{m\pm}\}$, $S_n^{m\pm}(t) = \sum_{k\in\mathcal{K}(n)} \{h(t)^k S_k^{m\pm}\}$, $n \in \mathbb{Z}_+$, and defines its gain matrices as $(Q_k^{m\pm} \in \mathbb{R}^{n_u \times n_x}$, $S_k^{m\pm} \in \mathbb{R}^{n_x \times n_x})$, which will be solved in Theorem

1. For the switch modes recorded as $m+$, one obtains: $h_m(t) = \max\{h_j(t),\ j \in \{1,\ldots,r\}\}$, $h_m(t) \geq \mu \sum_{i\in\{1,\ldots,r\},i\neq m} h_i(t)$. For the other ones recorded as $m-$, one obtains: $h_m(t) = \max\{h_j(t),\ j \in \{1,\ldots,r\}\}$, $h_m(t) < \mu \sum_{i\in\{1,\ldots,r\},i\neq m} h_i(t)$. Here, $\mu \geq 1$ is a flexible parameter about how to divide the entire state space into $2r$ switch modes with different sizes. The selection rule of μ will be illustrated by using several specific examples in Section IV.

Theorem 1: For the alert threshold of $\gamma > 0$, the closed-loop plant of (1) becomes asymptotically stabilizable via the the switching-type fuzzy state-feedback controller (6), if the given precondition of (5) is always satisfied and there are symmetric matrices $P_k \in \mathbb{R}^{n_x\times n_x}$, matrices $G_k^{m\pm} \in \mathbb{R}^{n_u\times n_x}$, $S_k^{m\pm} \in \mathbb{R}^{n_x\times n_x}$ with $(k \in \mathcal{K}(n)$; matrices $W_{pq}^m = (W_{qp}^m)^T \in \mathbb{R}^{2n_x\times 2n_x}$ and matrices $U_{pq}^m = (U_{qp}^m)^T \in \mathbb{R}^{2n_x\times 2n_x}$ with $m \in \{1,\ldots,r\}$, $p, q \in \mathcal{K}(s)$, $s \in \mathbb{Z}_+$; matrices $Z_{pq}^{mi} = (Z_{qp}^{mi})^T \in \mathbb{R}^{2n_x\times 2n_x}$ with $m, i \in \{1,\ldots,r\}$ and $i \neq m$, $p, q \in \mathcal{K}(s)$; such that all the linear matrix inequalities (LMIs) of (7)–(10) are fulfilled at the same time

$$\Gamma_{k'}^{m\pm} < 0 \quad \forall k' \in \mathcal{K}(\hat{n}) \tag{7}$$

$$\left[W_{pq}^m\right]_{J(s)\times J(s)} > 0 \tag{8}$$

$$\left[U_{pq}^m\right]_{J(s)\times J(s)} < 0 \tag{9}$$

$$\left[Z_{pq}^{mi}\right]_{J(s)\times J(s)} > 0 \tag{10}$$

where one defines $\hat{n} = \max\{n+1, 2s+1\}$. $[W_{pq}^m]_{J(s)\times J(s)}$, $[U_{pq}^m]_{J(s)\times J(s)}$, and $[Z_{pq}^{mi}]_{J(s)\times J(s)}$ belong to the augmented matrices developed in Section II-B. Furthermore, one also defines

$$\begin{aligned}\Gamma_{k'}^{m\pm} = &\sum_{k\in\mathcal{K}(n),k'\geq k}\left\{\phi_{kk'}\begin{bmatrix}\gamma P_k & * \\ 0 & -P_k\end{bmatrix}\right\} \\ &+ \sum_{\substack{k\in\mathcal{K}(n),j\in\{1,\ldots,r\}\\ k'\geq k+\chi_j}}\left\{\varphi_{kk'}^j\begin{bmatrix}-\mathrm{He}\left(S_k^{m\pm}\right) & * \\ A_jS_k^{m\pm}+B_jQ_k^{m\pm} & 0\end{bmatrix}\right\} \\ &+ \sum_{\substack{j\in\{1,\ldots,r\},p,q\in\mathcal{K}(s)\\ k'\geq p+q+\chi_j}}\frac{(\hat{n}-2s-1)!}{\pi(k'-p-q-\chi_j)}\Lambda_{pq}^{m\pm j}\end{aligned}$$

$$\phi_{kk'} = \frac{(\hat{n}-n)!}{\pi(k'-k)}, \varphi_{kk'}^j = \frac{(\hat{n}-n-1)!}{\pi(k'-k-\chi_j)}$$

$$\Lambda_{pq}^{m\pm j} = \begin{cases} W_{pq}^m, \text{ for switch modes } m+,\ j=m \\ -\mu W_{pq}^m, \text{ for switch modes } m+,\ j\neq m \\ U_{pq}^m + \sum_{i\in\{1,\ldots,r\},i\neq m} Z_{pq}^{mi} \\ \text{for switch modes } m-,\ j=m \\ -\mu U_{pq}^m - Z_{pq}^{mj}, \text{ for switch modes } m-,\ j\neq m. \end{cases}$$

Proof: Firstly, three key inequalities of (11)–(13) are derived by recalling (8)–(10) with $I \in \mathbb{R}^{2n_x\times 2n_x}$ and $\Omega = \begin{bmatrix} h(t)^{p^1}I \\ \vdots \\ h(t)^{p^{J(s)}}I \end{bmatrix}$

$$\sum_{p,q\in\mathcal{K}(s)} h(t)^{p+q}W_{pq}^m = \Omega^T\left[W_{pq}^m\right]_{J(s)\times J(s)}\Omega > 0 \tag{11}$$

$$\sum_{p,q\in\mathcal{K}(s)} h(t)^{p+q}U_{pq}^m = \Omega^T\left[U_{pq}^m\right]_{J(s)\times J(s)}\Omega < 0 \tag{12}$$

$$\sum_{p,q\in\mathcal{K}(s)} h(t)^{p+q}Z_{pq}^{mi} = \Omega^T\left[Z_{pq}^{mi}\right]_{J(s)\times J(s)}\Omega > 0. \tag{13}$$

All the possible switch modes $m\pm$ are classified as two categories: 1) switch modes recorded as $m+$ and 2) switch modes recorded as $m-$. If one of switch modes recorded as $m+$ is activated, one obtains $h_m(t) - \mu\sum_{(\substack{i\in\{1,\ldots,r\}\\ i\neq m})} h_i(t) \geq 0$ and thus

$$\left(h_m(t) - \mu\sum_{(\substack{i\in\{1,\ldots,r\}\\ i\neq m})} h_i(t)\right)\left(\sum_{p,q\in\mathcal{K}(s)} h(t)^{p+q}W_{pq}^m\right) \geq 0. \tag{14}$$

If one of switch modes recorded as $m-$ is activated, one obtains $h_m(t) - \mu\sum_{(\substack{i\in\{1,\ldots,r\}\\ i\neq m})} h_i(t) < 0$ and $(h_m(t) - h_j(t)) \geq 0$, and thus

$$\left(h_m(t) - \mu\sum_{(\substack{j\in\{1,\ldots,r\}\\ j\neq m})} h_j(t)\right)\left(\sum_{p,q\in\mathcal{K}(s)} h(t)^{p+q}U_{pq}^m\right) > 0 \tag{15}$$

$$\sum_{(\substack{j\in\{1,\ldots,r\}\\ j\neq m})}\left\{\left(h_m(t)-h_j(t)\right)\left(\sum_{p,q\in\mathcal{K}(s)} h(t)^{p+q}Z_{pq}^{mj}\right)\right\} \geq 0. \tag{16}$$

Next, using Property 1, one obtains

$$\begin{pmatrix}\gamma P_n(t) - \mathrm{He}\left(S_n^{m\pm}(t)\right) & * \\ A_{\varsigma(t)}S_n^{m\pm}(t) + B_{\varsigma(t)}Q_n^{m\pm}(t) & -P_n(t)\end{pmatrix} + \Lambda^{m\pm} = \sum_{k'\in\mathcal{K}(\hat{n})}\left\{h(t)^{k'}\Gamma_{k'}^{m\pm}\right\} \tag{17}$$

where $\Lambda^{m\pm} = \begin{cases}\text{Left(14)}, \text{ as } m+; \\ \text{Left(15)} + \text{Left(16)}, \text{ as } m-\end{cases}$, and $\Gamma_{k'}^{m\pm}$ is given in (7).

Therefore, the following inequality is guaranteed if (7)–(10) are fulfilled at the same time:

$$\begin{pmatrix}\gamma P_n(t) - \mathrm{He}(S_n^{m\pm}(t)) & * \\ A_{\varsigma(t)}S_n^{m\pm}(t) + B_{\varsigma(t)}Q_n^{m\pm}(t) & -P_n(t)\end{pmatrix} < 0. \tag{18}$$

Recalling $\gamma P_n(t) - \mathrm{He}(S_n^{m\pm}(t)) \geq -(S_n^{m\pm}(t))^T(\frac{1}{\gamma}P_n^{-1}(t))S_n^{m\pm}(t)$, one obtains,

$$\begin{pmatrix}-\left(S_n^{m\pm}(t)\right)^T\left(\frac{1}{\gamma}P_n^{-1}(t)\right)S_n^{m\pm}(t) & * \\ A_{\varsigma(t)}S_n^{m\pm}(t) + B_{\varsigma(t)}Q_n^{m\pm}(t) & -P_n(t)\end{pmatrix} < 0. \tag{19}$$

Pre and postmultiplying the above inequality of (19) with $\begin{pmatrix}S_n^{m\pm}(t) & 0 \\ 0 & P_n(t)\end{pmatrix}^{-T}$ and its transpose, one further obtains

$$\mathrm{He}\left(\Phi\begin{pmatrix}A_{\varsigma(t)} + B_{\varsigma(t)}Q_n^{m\pm}(t)\left(S_n^{m\pm}(t)\right)^{-1} & -I\end{pmatrix}\right) + \begin{pmatrix}-\frac{1}{\gamma}P_n^{-1}(t) & 0 \\ 0 & P_n(t)^{-1}\end{pmatrix} < 0 \tag{20}$$

where $\Phi = \begin{pmatrix}0 \\ P_n(t)^{-1}\end{pmatrix}$.

Therefore, using Lemma 1 here, the above inequality (20) produces

$$\xi(t,t+1)^T\begin{pmatrix}-\frac{1}{\gamma}P_n^{-1}(t) & 0 \\ 0 & P_n(t)^{-1}\end{pmatrix}\xi(t,t+1) < 0 \tag{21}$$

where $\xi(t,t+1) = \begin{pmatrix}x(t) \\ x(t+1)\end{pmatrix}$.

Based on (5), one obtains from (21)

$$\xi(t,t+1)^T\begin{pmatrix}-P_n^{-1}(t-1) & 0 \\ 0 & P_n(t)^{-1}\end{pmatrix}\xi(t,t+1) < 0. \tag{22}$$

If the Lyapunov function candidate is used to be

$$V(x(t), h(t-1)) = x^T(t)\left(\sum_{k\in\mathcal{K}(n)}\left\{h(t-1)^k P_k\right\}\right)^{-1} x(t) \quad (23)$$

then the forward difference $\Delta V(x(t), h(t-1))$ is guaranteed to be negative by considering (22). Therefore, the closed-loop plant of (1) becomes asymptotically stabilizable via the switching-type fuzzy state-feedback controller (6) if our proposed conditions of (7)–(10) are fulfilled at the same time. ■

Remark 2: Observed from both (5) and (7), there exists a tradeoff between the establishment of precondition (5) and the feasibility of (7), which is caused by the choice of γ. Therefore, it is meaningful for making the feasible stabilization region as large as possible while the same alert threshold is chosen as the recent result of [30]. Different from the recent result, the proprietary features of each switch mode recorded as $m\pm$ are exploited by exchanging positive/negative matrices [i.e., $(\sum_{p,q\in\mathcal{K}(s)} h(t)^{p+q} W^m_{pq})$, $(\sum_{p,q\in\mathcal{K}(s)} h(t)^{p+q} U^m_{pq})$ and $(\sum_{p,q\in\mathcal{K}(s)} h(t)^{p+q} Z^{mj}_{pq})$] among all the involved monomials of all the possible $\Gamma^{m\pm}_{k'}$ with $k' \in \mathcal{K}(\hat{n})$ and $m \in \{1, \ldots, r\}$. As a result, less conservative results of resilient fuzzy stabilization are obtained even if the higher alert thresholds are chosen for probably ensuring the establishment of precondition for resilient fuzzy stabilization, and this benefit will also be verified in the next section.

Remark 3: Furthermore, it should be noted that the other prescribed scalar $\mu \geq 1$ belongs to another influence factor of our newly developed result. Several different alternatives of μ can be chosen from $\{2, 3, 4, 5, 6, 7, \ldots\}$ and thus, the best μ is immediately found from the their variation tendency of the obtained results.

Remark 4: The main drawback of the proposed method is that the number of required gain matrices $Q^{m\pm}_k$ and $S^{m\pm}_k$ increases by $2r$ times as the original number of [30]. That is, a larger storage space (more than $2r$ times) is needed in the real world in order to implement the switching-type fuzzy state-feedback controller (6). In other words, there exists a tradeoff between better control performance and more expensive cost of realization.

Remark 5: The reason for why only TS fuzzy type is considered is that most of related literature are based on TS fuzzy models, such as [25]–[30]. In fact, the main contributions of this technical correspondence focus on how to make good use of NFWFs [see (15)–(17) for details]. Considering the fact that NFWFs belong to the essential components of all kinds of fuzzy models, the developed results can be extended to other fuzzy types as well, for example, Mamdani or Tsukomot types.

IV. Numerical Simulation

Example: Consider the well-known benchmark example for (1) with $h_1(v(t)) = (\delta + x_1(t))/2\delta$, $h_2(v(t)) = (\delta - x_1(t))/2\delta$, and $A_1 = \begin{bmatrix} 1.0 & -\delta \\ -1.0 & -0.5 \end{bmatrix}$, $B_1 = \begin{bmatrix} 5.0+\delta \\ 2\delta \end{bmatrix}$, $A_2 = \begin{bmatrix} 1.0 & \delta \\ -1.0 & -0.5 \end{bmatrix}$, and $B_2 = \begin{bmatrix} 5.0-\delta \\ -2\delta \end{bmatrix}$. As that pointed out in [20], the feasible stabilization region is proportional to the maximal value of δ (which is denoted as $\delta_{\max}$). Here, an intuitive explanation of the theoretical meaning of $(\delta_{\max}, \gamma, \mu)$ is given as follows. $\delta_{\max}$ is directly proportional to the range of feasible stabilization region, the alert threshold γ is directly proportional to the possibility for probably ensuring the establishment of the precondition of resilient fuzzy stabilization (5), and μ is a flexible parameter about how to divide the entire state space into $2r$ switch modes with different sizes. In other words, our first aim is to provide the maximal $\delta_{\max}$ by adjusting different μ while the same alert threshold γ is chosen as the recent one [30].

TABLE I
Solvable $\delta_{\max}$ of Theorem 1 With $\mu \in \{2, 3, 4, 5, 6, 7\}$ and $\gamma \in \{2, 3, 4, 5\}$, Respectively

γ/μ	2	3	4	5	6	7
2	3.268	3.281	3.295	3.307	3.316	3.316
3	2.603	2.639	2.646	2.646	2.646	2.646
4	2.170	2.185	2.185	2.185	2.185	2.185
5	1.957	1.962	1.962	1.962	1.962	1.962

TABLE II
Comparisons of Solvable $\delta_{\max}$ for [27]–[30] and Theorem 1 With $\gamma \in \{2, 3, 4, 5\}$ and $\mu = 2$

γ	2	3	4	5
[27]	1.768	1.768	1.768	1.768
[28]	1.806	1.806	1.806	1.806
[29]	1.819	1.819	1.819	1.819
[30]	2.180	1.792	1.537	1.377
Best[27]–[30]	2.180	1.819	1.819	1.819
Ours	3.268	2.603	2.170	1.957
increase rate	49.9% ↑	43.1% ↑	19.3% ↑	7.6% ↑

Without loss of generality, using the identical degrees of gain matrices ($n = 2$ for Theorem 1) as the existing ones of [29] and [30], all the solvable $\delta_{\max}$ of Theorem 1 with $\mu \in \{2, 3, 4, 5, 6, 7\}$ and $\gamma \in \{2, 3, 4, 5\}$ are presented in Table I. Through careful observation of Table I, two main conclusions can be obtained for this case study: 1) for each fixed μ, the solvable $\delta_{\max}$ becomes more and more larger as the chosen value of γ becomes smaller, and this shows that there exists a tradeoff between $\delta_{\max}$ and γ and 2) for each fixed γ, the solvable $\delta_{\max}$ reaches the local optimal solution as the value of μ is chosen as a bigger value such as $\mu = 6$ or 7, and this shows that the better $\delta_{\max}$ can be obtained by adjusting μ from the finite set of $\mu \in \{2, 3, 4, 5, 6, 7\}$. Since those conventional fuzzy stabilization methods (e.g., [27]–[29] and so on) are reported to be unable to obtain any feasible stabilization region such that $\delta_{\max} > 1.830$, it is important to point out that our proposed resilient fuzzy stabilization is superior to the conventional fuzzy stabilization with regard to enlarging the feasible stabilization region. Nevertheless, one smaller γ does make the given Assumption 1 more difficult to be guaranteed, and thus, it is very meaningful for further enlarging the solvable $\delta_{\max}$ as large as possible while the same alert threshold of γ is chosen as the recent one of [30].

Next, the result of the study will be compared with those existing results of [27]–[29] and [30] together. First, the comparisons of solvable $\delta_{\max}$ for [27]–[30] and Theorem 1 with $\gamma \in \{2, 3, 4, 5\}$ and $\mu = 2$ have been listed in Table II. For each fixed γ, the solvable $\delta_{\max}$ of the study is larger than the other ones given in [27]–[30]. Moreover, compared to the best results given in [27]–[30], the maximal increase rate even exceeds 49.9% as $\gamma = 2$ while the minimal increase rate exceeds 7.6% as $\gamma = 5$. That is to say, the feasible stabilization region has been well enlarged while the same alert threshold of γ is chosen as before. Second, in order to given a visual display, Fig. 1 is provided in which two evolution trends of $\delta_{\max}$ along different γ for [30] and this article are displayed while $\delta_{\max} = 1.830$ is the ultimate limit of those conventional methods such as [27]–[29]. Appreciably, our result of the dark blue solid line can be beyond the ultimate limit of those conventional methods within the entire interval of $1 \leq \gamma \leq 5$, but the recent result of the blue-dotted line given by [30] is under than the red line of $\delta_{\max} = 1.830$ within the second half of the entire interval. Therefore, it is reasonable to say

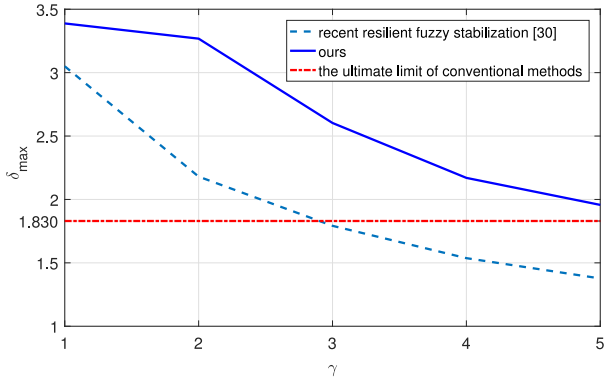

Fig. 1. Two evolution trends of $\delta_{\max}$ along different γ for [30] and this article while $\delta_{\max} = 1.830$ is the ultimate limit of those conventional methods such as [27]–[29].

that less conservative results have been obtained even if some higher alert thresholds are chosen for probably ensuring the establishment of the involved precondition.

When δ is selected as $\delta = 3.268$, one notices that the investigated system is out of any feasible stabilization region of [27]–[30] by observing Table II. However, the investigated system is within the feasible stabilization region of Theorem 1 with $n = 2$, $\gamma = 2$, and $\mu = 2$. Furthermore, our designing conditions of (7)–(10) are solved and the following gain matrices of $(S_k^{m\pm}, Q_k^{m\pm})$ with $m \in \{1, 2\}$ and $k \in \{20, 11, 02\}$ are acquired.

$m\pm = 1+$ is called as the 1st switch mode

$$S_{20}^{1+} = \begin{bmatrix} 0.2034 & 0.1877 \\ 0.1710 & 0.1584 \end{bmatrix}$$
$$S_{11}^{1+} = \begin{bmatrix} -0.5280 & -0.3519 \\ 0.0226 & 0.1666 \end{bmatrix}$$
$$S_{02}^{1+} = \begin{bmatrix} 0.5786 & 0.0129 \\ -0.0949 & -0.0105 \end{bmatrix}$$
$$Q_{20}^{1+} = \begin{bmatrix} 0.0336 & 0.0330 \end{bmatrix}$$
$$Q_{11}^{1+} = \begin{bmatrix} -0.0285 & 0.0172 \end{bmatrix}$$
$$Q_{02}^{1+} = \begin{bmatrix} -0.0450 & -0.0155 \end{bmatrix}.$$

$m\pm = 1-$ is called as the 2nd switch mode

$$S_{20}^{1-} = \begin{bmatrix} 0.2095 & 0.2540 \\ 0.1634 & 0.1817 \end{bmatrix}$$
$$S_{11}^{1-} = \begin{bmatrix} -0.5559 & -0.4981 \\ 0.0915 & 0.2354 \end{bmatrix}$$
$$S_{02}^{1-} = \begin{bmatrix} 0.6066 & 0.1401 \\ -0.2246 & -0.0046 \end{bmatrix}$$
$$Q_{20}^{1-} = \begin{bmatrix} 0.0351 & 0.0363 \end{bmatrix}$$
$$Q_{11}^{1-} = \begin{bmatrix} -0.0302 & 0.0286 \end{bmatrix}$$
$$Q_{02}^{1-} = \begin{bmatrix} -0.0505 & -0.0383 \end{bmatrix}.$$

$m\pm = 2+$ is called as the 3rd switch mode

$$S_{20}^{2+} = \begin{bmatrix} 0.7200 & -0.0076 \\ 0.2475 & -0.0043 \end{bmatrix}$$
$$S_{11}^{2+} = \begin{bmatrix} -0.7326 & -0.3500 \\ 0.0602 & 0.2599 \end{bmatrix}$$
$$S_{02}^{2+} = \begin{bmatrix} 0.6889 & -0.0447 \\ -0.2874 & 0.0868 \end{bmatrix}$$
$$Q_{20}^{2+} = \begin{bmatrix} -0.0009 & 0.0301 \end{bmatrix}$$
$$Q_{11}^{2+} = \begin{bmatrix} -0.0191 & 0.0424 \end{bmatrix}$$
$$Q_{02}^{2+} = \begin{bmatrix} -0.0882 & 0.0035 \end{bmatrix}.$$

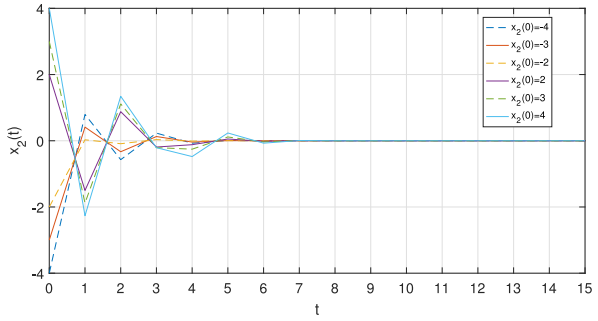

Fig. 2. Six trajectories of $x_2(t)$ of cases I–VI.

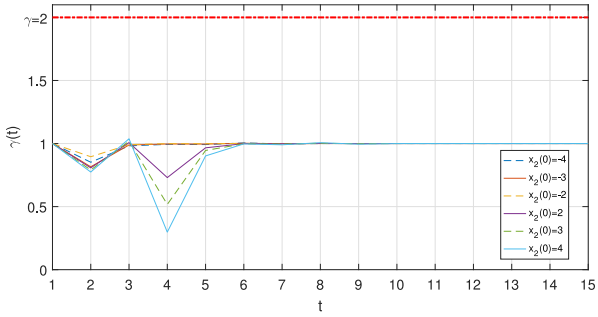

Fig. 3. Six trajectories of $\gamma(t)$ of cases I–VI.

$m\pm = 2-$ is called as the 4th switch mode

$$S_{20}^{2-} = \begin{bmatrix} 0.2542 & 0.1235 \\ 0.0362 & 0.1641 \end{bmatrix}$$
$$S_{11}^{2-} = \begin{bmatrix} -0.6797 & -0.3025 \\ 0.3937 & 0.0995 \end{bmatrix}$$
$$S_{02}^{2-} = \begin{bmatrix} 0.7720 & -0.0915 \\ -0.3935 & 0.1361 \end{bmatrix}$$
$$Q_{20}^{2-} = \begin{bmatrix} 0.0108 & 0.0280 \end{bmatrix}$$
$$Q_{11}^{2-} = \begin{bmatrix} 0.0502 & 0.0161 \end{bmatrix}$$
$$Q_{02}^{2-} = \begin{bmatrix} -0.1236 & 0.0148 \end{bmatrix}.$$

Moreover, three matrices of P_{20}, P_{11}, and P_{02} for constructing our Lyapunov function candidate of (23) have also been provided

$$P_{20} = \begin{bmatrix} 0.1813 & 0.1622 \\ 0.1622 & 0.1451 \end{bmatrix}$$
$$P_{11} = \begin{bmatrix} -0.5209 & -0.1599 \\ -0.1599 & 0.1645 \end{bmatrix}$$
$$P_{02} = \begin{bmatrix} 0.4673 & -0.0479 \\ -0.0479 & 0.0192 \end{bmatrix}.$$

In order to show its control effect, six different $x_2(0)$ have been applied in unison with $x_1(0) = 0.6$: case I: $x_2(0) = -4.0$, case II: $x_2(0) = -3.0$, case III: $x_2(0) = -2.0$, case IV: $x_2(0) = 2.0$, case V: $x_2(0) = 3.0$, and case VI: $x_2(0) = 4.0$.

Using the switching-type fuzzy state-feedback controller of (6), six responses of $x_2(t)$ for cases I–VI have been given in Fig. 2 and six responses of $\gamma(t) = ([x^T(t)(P_n(t))^{-1}x(t)]/[x^T(t)(P_n(t-1))^{-1}x(t)])$ for cases I–VI have been given in Fig. 3. Since all the six $x_2(t)$ are asymptotically stable and $\gamma(t) \leq \gamma = 2$ (Assumption 1) is evidently ensured, it can be said that much less conservative results of resilient fuzzy stabilization have been obtained while the establishment of precondition for resilient fuzzy stabilization (5) is well ensured for all the six cases. Without loss of generality, the trajectory of $u(t)$ and the actual modes $m\pm$ of case VI have also been shown in Fig. 4. It can be found that $m\pm = 1-$ and $m\pm = 2-$ have been enabled in the

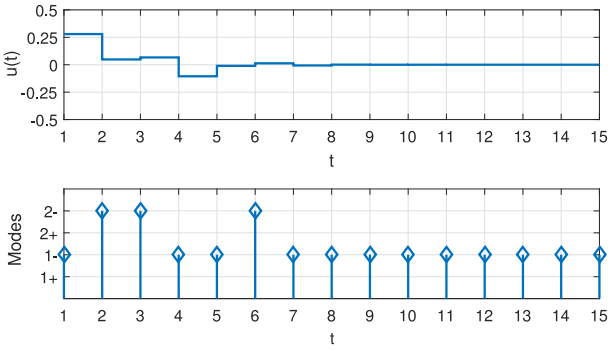

Fig. 4. Trajectory of $u(t)$ and the actual modes $m\pm$ of case VI.

first interval $1 \leq t \leq 6$ and the activated mode stays at $m\pm = 1-$ in the second half $7 \leq t \leq 15$.

V. Conclusion

The resilient fuzzy stabilization has been well enhanced in the direction of enlarging the feasible stabilization region as large as possible for each fixed alert threshold of γ. Different from the recent one of [30], the switching-type fuzzy state-feedback controller has been designed with different gain matrices for each switch mode. Based on this, a novel augmented time-variant matrix approach has been proposed in order to exploit proprietary features of each switch mode via exchanging positive/negative matrices among all the involved monomials to full advantage. Consequently, less conservative results have been obtained even if the higher alert thresholds are chosen for probably guaranteeing the establishment of $\gamma(t) \leq \gamma$ all the way. The superiority of our approach has been validated by providing some detailed comparisons on the benchmark example. Future work includes resilient control synthesis of fuzzy systems with practical state and input constraints, in which much more proprietary features of NFWFs are required to be excavated and applied by developing new measures.

References

[1] H. Zhang, Y. Mun, Z. Gao, and W. Wang, "Observer-based fault reconstruction and fault-tolerant control for nonlinear systems subject to simultaneous actuator and sensor faults revised manuscript for TFS-2020-1045," *IEEE Trans. Fuzzy Syst.*, early access, Jul. 21, 2021, doi: 10.1109/TFUZZ.2021.3098341.

[2] H. Zhang, Y. Liu, and Y. Wang, "Observer-based finite-time adaptive fuzzy control for nontriangular nonlinear systems with full-state constraints," *IEEE Trans. Cybern.*, vol. 51, no. 2, pp. 1110–1120, Mar. 2021.

[3] J. Sun, H. Zhang, Y. Wang, and S. Sun, "Fault-tolerant control for stochastic switched IT2 fuzzy uncertain time-delayed nonlinear systems," *IEEE Trans. Cybern.*, vol. 52, no. 2, pp. 1335–1346, Feb. 2022, doi: 10.1109/TCYB.2020.2997348.

[4] H. Wang, W. Bai, X. Zhao, and P. X. Liu, "Finite-time prescribed performance-based adaptive fuzzy control for strict-feedback nonlinear systems with dynamic uncertainty and actuator faults," *IEEE Trans. Cybern.*, early access, Jan. 15, 2021, doi: 10.1109/TCYB.2020.3046316.

[5] L. Liu, T. Gao, Y.-J. Liu, S. Tong, C. L. P. Chen, and L. Ma, "Time-varying IBLF based on adaptive control of uncertain nonlinear systems with full state constraints," *Automatica*, vol. 129, Jul. 2021, Art. no. 109595.

[6] Q. Zheng, S. Xu, and B. Du, "Quantized guaranteed cost output feedback control for nonlinear networked control systems and its applications," *IEEE Trans. Fuzzy Syst.*, early access, May 21, 2021, doi: 10.1109/TFUZZ.2021.3082691.

[7] T. Takagi and M. Sugeno, "Fuzzy identification of systems and its applications to modeling and control," *IEEE Trans. Syst., Man, Cybern.*, vol. SMC-15, no. 1, pp. 116–132, Jan./Feb. 1985.

[8] H. Li, Y. Y. Wu, M. Chen, and R. Lu, "Adaptive multigradient recursive reinforcement learning event-triggered tracking control for multi-agent systems," *IEEE Trans. Neural Netw. Learn. Syst.*, early access, Jul. 1, 2021, doi: 10.1109/TNNLS.2021.3090570.

[9] F. Li, P. Shi, C.-C. Lim, and L. Wu, "Fault detection filtering for nonhomogeneous Markovian jump systems via a fuzzy approach," *IEEE Trans. Fuzzy Syst.*, vol. 26, no. 1, pp. 131–141, Feb. 2018.

[10] X.-H. Chang, J. H. Park, and P. Shi, "Fuzzy resilient energy-to-peak filtering for continuous-time nonlinear systems," *IEEE Trans. Fuzzy Syst.*, vol. 25, no. 6, pp. 1576–1588, Dec. 2017.

[11] X.-M. Zhang, Q.-L. Han, and X. Ge, "A novel finite-sum inequality-based method for robust control of uncertain discrete-time Takagi-Sugeno fuzzy systems with interval-like time-varying delays," *IEEE Trans. Cybern.*, vol. 48, no. 9, pp. 2569–2582, Sep. 2018.

[12] T. Zhao and S. Dian, "State feedback control for interval type-2 fuzzy systems with time-varying delay and unreliable communication links," *IEEE Trans. Fuzzy Syst.*, vol. 26, no. 2, pp. 951–966, Apr. 2018.

[13] R.-E. Precup and H. Hellendoorn, "A survey on industrial applications of fuzzy control," *Comput. Ind.*, vol. 62, no. 3, pp. 213–226, 2011.

[14] J. Dong, Q. Hu, M. Ren, "Control synthesis for discrete-time T-S fuzzy systems based on membership function-dependent H_∞ performance," *IEEE Trans. Fuzzy Syst.*, vol. 28, no. 12, pp. 3360–3366, Dec. 2020.

[15] D. H. Lee and J. Hu, "Local model predictive control for T–S fuzzy systems," *IEEE Trans. Cybern.*, vol. 47, no. 9, pp. 2556–2567, Sep. 2017.

[16] L.-K. Wang, J. Liu, and H.-K. Lam, "New results of observer design for continuous-time fuzzy systems: A switching technique," *IEEE Trans. Syst., Man, Cybern., Syst.*, early access, Dec. 14, 2021, doi: 10.1109/TSMC.2021.3132372.

[17] P. Baranyi, "The generalized TP model transformation for T-S fuzzy model manipulation and generalized stability verification," *IEEE Trans. Fuzzy Syst.*, vol. 22, no. 4, pp. 934–948, Aug. 2014.

[18] W. Ji, J. Qiu, and H.-K. Lam, "A new sampled-data output-feedback controller design of nonlinear systems via fuzzy affine models," *IEEE Trans. Cybern.*, vol. 52, no. 2, pp. 1681–1690, Mar. 2022.

[19] V. C. Campos, F. O. Souza, L. A. Torres, and R. M. Palhares, "New stability conditions based on piecewise fuzzy Lyapunov functions and tensor product transformations," *IEEE Trans. Fuzzy Syst.*, vol. 21, no. 4, pp. 748–760, Aug. 2013.

[20] T. M. Guerra and L. Vermeiren, "LMI-based relaxed nonquadratic stabilization conditions for nonlinear systems in the Takagi-Sugeno's form," *Automatica*, vol. 40, no. 5, pp. 823–829, 2004.

[21] D. H. Lee, J. B. Park, and Y. H. Joo, "Improvement on nonquadratic stabilization of discrete-time Takagi-Sugeno fuzzy systems: Multiple-parameterization approach," *IEEE Trans. Fuzzy Syst.*, vol. 18, no. 2, pp. 425–429, Apr. 2010.

[22] D. H. Lee, J. B. Park, and Y. H. Joo, "Approaches to extended nonquadratic stability and stabilization conditions for discrete-time Takagi-Sugeno fuzzy systems," *Automatica*, vol. 47, no. 3, pp. 534–538, 2011.

[23] R. C. L. F. Oliveira and P. L D. Peres, "Parameter-dependent LMIs in robust analysis: Characterization of homogeneous polynomially parameter-dependent solutions via LMI relaxations," *IEEE Trans. Autom. Control*, vol. 52, no. 7, pp. 1334–1340, Jul. 2007.

[24] B. C. Ding, "Homogeneous polynomially nonquadratic stabilization of discrete-time Takagi-Sugeno systems via nonparallel distributed compensation law," *IEEE Trans. Fuzzy Syst.*, vol. 18, no. 5, pp. 994–1000, Oct. 2010.

[25] Z. Lendek, T. M. Guerra, and J. Lauber, "Controller design for TS models using delayed nonquadratic Lyapunov functions," *IEEE Trans. Cybern.*, vol. 45, no. 3, pp. 453–464, Mar. 2015.

[26] X. Xie, D. Yue, H. Zhang, and Y. Xue, "Control synthesis of discrete-time T-S fuzzy systems via a multi-instant homogenous polynomial approach," *IEEE Trans. Cybern.*, vol. 46, no. 3, pp. 630–640, Mar. 2016.

[27] X. Xie, D. Yue, and C. Peng, "Relaxed real-time scheduling stabilization of discrete-time Takagi–Sugeno fuzzy systems via a alterable-weights-based ranking switching mechanism," *IEEE Trans. Fuzzy Syst.*, vol. 26, no. 6, pp. 3808–3819, Dec. 2018.

[28] P. H. S. Coutinho, J. Lauber, M. Bernal, and R. M. Palhares, "Efficient LMI conditions for enhanced stabilization of discrete-time Takagi-Sugeno models via delayed nonquadratic Lyapunov functions," *IEEE Trans. Fuzzy Syst.*, vol. 27, no. 9, pp. 1833–1843, Sep. 2019.

[29] X. Xie, C. Bu, and C. Peng, "Multi-instant gain-scheduling stabilization of discrete-time Takagi-Sugeno fuzzy systems based on a time-variant balanced matrix approach," *IEEE Trans. Fuzzy Syst.*, early access, Jun. 14, 2021, doi: 10.1109/TFUZZ.2021.3089047.

[30] X. Xie, J. Lu, and D. Yue, "Resilient stabilization of discrete-time Takagi-Sugeno fuzzy systems: Dynamic trade-off between conservatism and complexity," *Inf. Sci.*, vol. 582, pp. 181–197, Jan. 2022.

[31] R. E. Skelton, T. Iwasaki, and K. Grigoriadis, *A Unified Approach to Linear Control Design*. London, U.K.: Taylor Francis, 1998.